

# Adaptive Sampling Algorithms for Multiple Autonomous Underwater Vehicles

Dan O. Popa<sup>†</sup> Arthur C. Sanderson<sup>†</sup> Rick Komerska<sup>‡</sup>  
Sai Mupparapu<sup>‡</sup> Richard Blidberg<sup>‡</sup> and Steven Chappel<sup>‡</sup>

<sup>†</sup>Rensselaer Polytechnic Institute, Troy, New York

<sup>‡</sup>Autonomous Undersea Systems Institute (AUSI), Lee, New Hampshire

**Abstract** - Sampling is a critical problem in the observation of underwater phenomena using single or multiple AUV platforms. The determination of optimal paths and sampling strategies that effectively utilize available resources is critical to these missions. Recent work performed jointly at RPI and AUSI on the development of Adaptive Sampling Algorithms (ASA) utilizes information measures, estimation theory, and potential fields to direct the robots to the locations in space most likely to yield information about the sensed field variable of interest. Typical sensory information can consist of spatial distribution of one or more field variables, such as salinity, dissolved oxygen, temperature, current, etc. In order to test our algorithms we have created the MATCON simulation environment, an underwater experimental platform using solar AUVs, and a land-based experimental testbed using inexpensive wheeled robots.

## I. INTRODUCTION

Recently, there has been renewed interest in using mobile robots on land, under water and in air, as sensor carrying platforms in order to perform sampling missions, such as searching for harmful biological and chemical agents, search and rescue in disaster areas, or environmental mapping and monitoring [1,2,17,18,23]. Even though mobility introduces additional degrees of complexity in managing an untethered collection of vehicles, it allows the repositioning of the on-board sensors. This, in turn, can greatly expand the coverage and survivability of the sensor network. In the context of autonomous underwater vehicles, many important issues regarding the deployment architecture await to be fully addressed, including the AUV size, cost, and coverage tradeoff, the selection of appropriate information measures to guide and evaluate the mission, and the distribution of computation and communication among the autonomous vehicles. Sampling is a broad methodology for gathering statistics about physical and social phenomena, and it provides a data source for predictive modeling in oceanography and meteorology [28-36].

Adaptive sampling denotes sampling strategies that can change depending on prior measurements or analysis, and thus allow for adaptation to dynamic or unknown scenarios. One such scenario involves the deployment of multiple underwater vehicles for the environmental monitoring of large bodies of water, such as oceans, harbors, lakes, rivers and estuaries. Predictive models and maps can be created by repeated measurements of physical characteristics such as water temperature, dissolved oxygen, current strength and direction, or bathymetry. However, because the sampling volume could be quite large, only a limited number of

measurements are usually available. Intuitively, a deliberate sampling strategy based on models will be more efficient than just a random sampling strategy.

In this paper we aim to define what constitute good measures of sampling efficiency, and use these measures to generate the sampling mission for multiple underwater vehicles. A variety of factors are considered, including localization and field variable uncertainties, energy and sampling time constraints, physical constraints such as nonholonomic vehicles or obstacles in the search space, as well as a limited communication bandwidth between the vehicles.

## II. BACKGROUND

Extensive research has been done in the area of cooperative goal attainment using multiple robots, either in the context of cooperative manipulation [8], as well as robot team behavior [9-13]. Some of this research is based on behavioral robotics [14], cooperative mapping and localization [15], multi-robot motion planning [12], and multi-sensor fusion [16]. Many examples of robot team tasks have been investigated on a variety of hardware platforms, for example foraging, ant colony behavior, robotic soccer, map making, area searching, mine sweeping, etc. In [9], probabilistic target points are assigned to robots to reduce exploration time, and in [7] robots are utilized as landmarks for localization.

The problem of multiple robot localization has also been extensively addressed using Monte Carlo and Markov chain stochastic estimation, and the Kalman Filter [15,45]. In the case of underwater vehicles, local navigation sensor readings (inertial, speed, etc) are fused with infrequent GPS fixes when the vehicle is on the surface, as well as range measurements using sonar to other underwater vehicles or fixed buoys. Mobile navigation algorithms have often been used with robot team objectives such as coverage or mapping of an unknown environment [12,13].

While multiple AUV localization is a classic problem in robotic, the problem of distributed field variable estimation is typically relevant to charting and prediction in oceanography and meteorology [30-36]. The typical modeling approach involves finding a partial differential equation and corresponding boundary conditions to express the evolution of the field variables in the 4D position-time space. This type of model fitting has also been referred to as “inverse modeling”, e.g. finding a functional solution for a set of given observation samples. In this context, measurement

uncertainty has also been addressed using Kalman-filter estimation techniques [44].

Another associated problem that has been previously investigated is the problem of stochastic tracking. The typical application includes the estimation for the position of a moving target through range measurements from several fixed locations. As the object moves through the sensor field, range data from various sensors is fused using either stochastic or Kalman filter estimation approaches [52].

Some of the goal attaining/team behavior research relevant to our sampling problem has been addressed using potential fields, in particular obstacle avoidance or goal attainment schemes often use penalty functions to bend feasible paths around obstacles, or to reposition holonomic or nonholonomic wheeled robots at an end point attractor, such as it was originally presented by Krogh [4] and Khatib [37]. Path planning algorithms for mobile robots now routinely employ potential fields [19, 20]. In [30] robot group uniformity is maintained through the use of artificial potentials. As with many optimization schemes, it is difficult to prove convergence of the performance index (potential function) to a global minimum, due to the presence of singularities [35]. Thus, a combination of global and local optimization methods is normally used.

Extensive research has also been done in the context of ad-hoc sensor networks, in particular in finding heuristic, sub-optimal solutions for network routing [3], deployment [21,27], and congestion control [6,7]. The congestion control problem consists of setting both the source and link controls of the network to ensure that the data rates and node buffers remain stable and converge to their static optimal values. A general passivity framework has been proposed in [7] as a superset solution for flow control.

Several wireless network protocols have been formulated using the above concepts, such as IEEE 802.11a,b, Bluetooth and PAMAS, and some of them specifically apply to sensor networks, such as PICONET and SMAC [24]. Since these protocols target RF networks, they can only be used if the AUVs are on the surface. Previous research in underwater acoustic networks has resulted in protocols such as Seaweb, FRONT, or AUSNET [43].

### III. MULTIPLE AUV PLATFORMS

#### A. Experimental AUV platform

The Solar vehicle SAUV-II designed by AUSI and built by Falmouth Scientific (FSI), is shown in Figure 5 [37-39]. This vehicle is being used as the principal experimental platform for the development and testing of ASA algorithms. A preliminary sampling mission with a single vehicle was recently conducted in Lake George, NY, at the Darrin Freshwater Institute of Rensselaer Polytechnic Institute at Bolton Landing, New York, in June, 2004, and successfully tested the command, control, communication, and sensor tools of the vehicle.

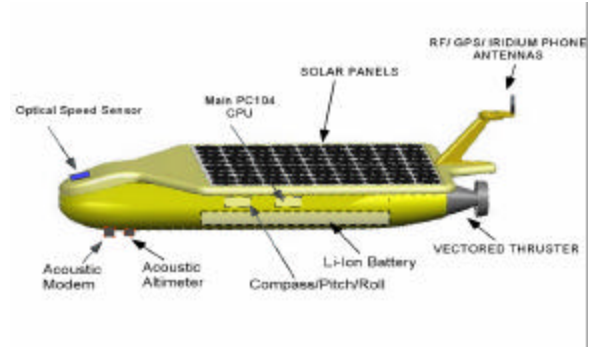


Fig. 5: Subsystems of AUSI's SAUV-II.

In the next set of experimental measurements using multiple vehicles, bathymetry and dissolved oxygen in the lake will be taken by multiple SAUV's, as well as static Russ buoy sensors shown in Figure 6. The goal is to chart the distribution of the sensed variables in a several square mile region of the lake.



Fig. 6: Sensor-based monitoring system (RUSS, Apprise Technology Inc.) in use at Rensselaer's Darrin Fresh Water Institute

#### B. MATCON, an estimation-friendly simulation environment

As an aid to our investigations of multiple cooperating vehicles with Adaptive Sampling Algorithms (ASA) we have enhanced the CADCON [40,42] simulation tool, and provided an interface with MATLAB.

As a stand-alone simulator, CADCON employs a distributed multi-agent simulation, visualization system, and control harness designed to simulate underwater environment, which can be shared via the Internet (Figure 1). The CADCON clients are available via the Internet for others to use and it has been employed by independent workers in industry and academia to support their own research projects. Through a DLL interface to MATLAB, an ASA algorithm written in MATLAB and running on a computer in Troy, New York, can be used to direct a fleet of simulated underwater vehicles on a sampling mission. The adaptive sampling algorithm, interfaces to a CADCON client, AUVSim (controls the vehicle behavior), using a DLL. The AUVSim is connected over the internet to CADCON simulation environment, running on a server located in Lee, New Hampshire. The applications share AUV's location and on-board sensory information: desired sampling locations for AUVs are then sent to CADCON for motion execution, path

planning, and visualization. Visualization is done using the CADCON client Visualizer, which also connects to the CADCON server over the internet.

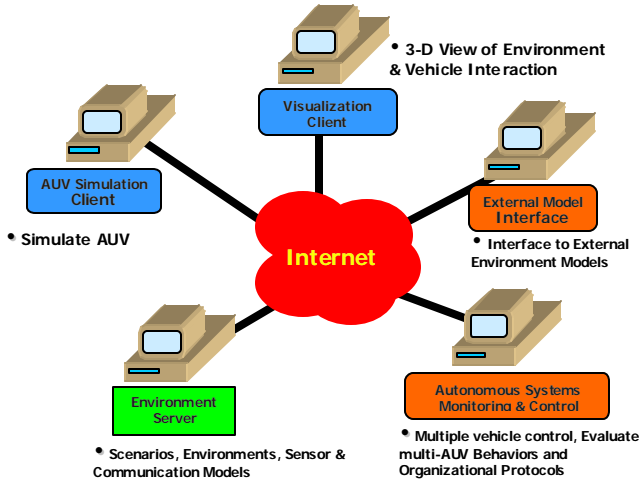


Fig. 1. CADCON Components linked through the Internet

Multiple AUVs can be instantiated and visualized using CADCON, and a high degree of detailed functional specs can be customized for each vehicle: energy available, sensor types, turning radius, etc (Figure 2). One of the simulated AUV models is the Solar AUV II underwater vehicle [38].

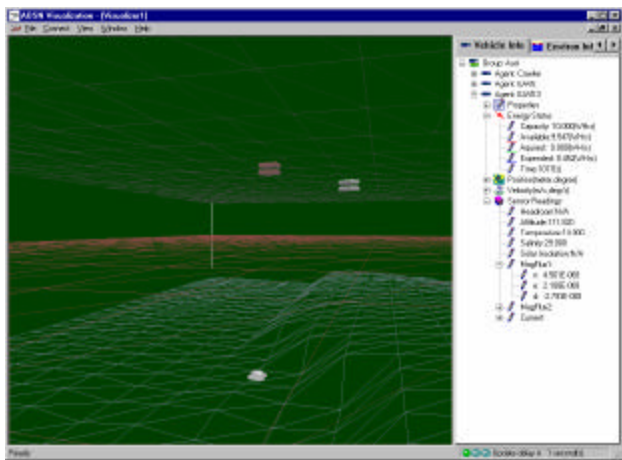


Fig. 2. CADCON visualizer screen capture of multiple AUV instances inside the simulation environment.

During the actual mission, the ASA utilizes the ASMAC environment (Autonomous Systems Monitoring and Control for a fleet of AUVs) to direct a fleet of AUVs to sampling locations. ASMAC allows a remote user to plan a mission, configure the AUVs that are going to accomplish that mission, initiate the mission, monitor the mission while it is underway, analyze received mission data and vehicle status and, as a result of that analysis, modify the mission while it is underway [42]. The collected sensor data is analyzed by ASA, which generates an output that helps re-plan the mission to better achieve the goals of the mission.

Another component of the simulation environment is the use of netCDF as a common database format to facilitate the

importing of real and simulated data into the simulator. Unidata's netCDF (Network Common Data Form) is a data model for array-oriented scientific data access, freely available software that implements the data model in several programming languages, and a machine-independent file format [41]. Since we would like to estimate a field distribution, we are interested in so called “plume” data, and we use the netCDF data format to describing its space-time evolution in both CADCON and MATLAB. Figure 3 shows the visual aspect of a simulated plume in both environments. The plume is generated using a “chimney” model that utilizes a diffusion differential equation on two coordinates, and a flow differential equation on the third coordinate. We use publicly available C and MATLAB code to perform I/O with netCDF data in both the CADCON environment server as well as MATLAB.

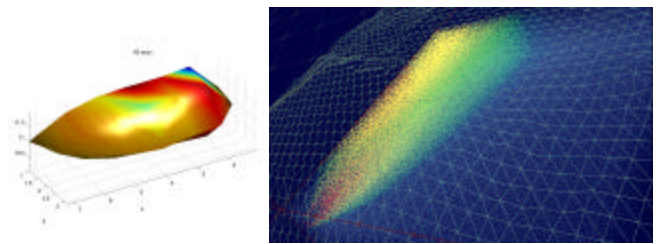


Fig. 3. Graphical representation of a simulated plume in MATLAB (left) and CADCON (right).

A diagram of MATCON, i.e. the overall simulation environment, is shown in Figure 4. Estimation-based ASA algorithms can now be easily implemented through the use of the optimization and estimation toolboxes in MATLAB.

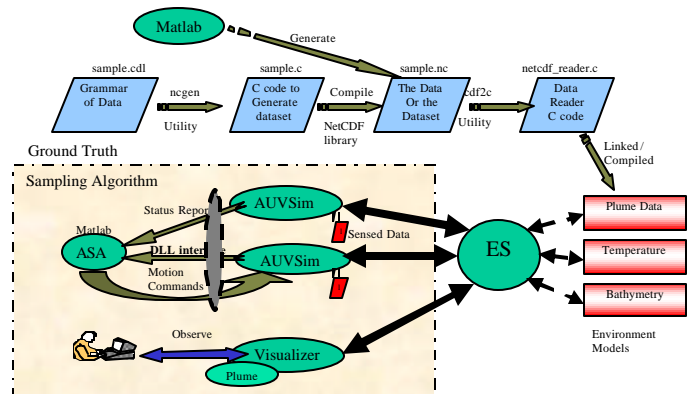


Fig. 4. Schematic diagram of MATCON, an estimation-friendly simulation environment for adaptive sampling.

## IV. ADAPTIVE SAMPLING ALGORITHMS

### A. Problem formulation

We define the generic Adaptive Sampling problem as follows:

Given  $N$  underwater vehicles sampling a space-time field distribution, where should the vehicles be directed to sample such that:

- ? The uncertainty in the knowledge of the field distribution is minimized.
- ? Network utilization is optimized given bandwidth constraints between vehicles that vary with the distance between them.
- ? Additional secondary objectives, such as minimizing energy consumption, obstacle avoidance, and sampling duration are minimized.

Addressing the AS problem involves four different aspects depicted in Figure 7.

- ? Field variable estimation using adaptive sampling.
- ? Sensor/robot localization using SLAM-type of algorithms [44].
- ? Robot repositioning in the presence of physical and energy constraints.
- ? Optimization of communication protocol during reconfiguration.

The primary contribution of our work is the combination of uncertainty in localization as well as in the sensor measurements. Both these uncertainties are especially relevant for underwater vehicles, since position estimates are often inaccurate due to navigational errors from dead-reckoning. Our approach is based on model parameter estimation for the field variable, which we then use as an additional constraint for reducing the uncertainty in the AUV localization. For example, if the field distribution is a linear function of the sample location, and assuming that two of the sample coordinates can be measured accurately while the third one is inaccurate, one can certainly determine the third coordinate from the additional constraint imposed by the field distribution.

### B. Information Measures and the Kalman Filter

Let  $X_i[k]$  denote the 3D position of the  $i$ -th AUV at sample number  $k$ . Assuming that a kinematic model for the AUV is a sufficiently accurate representation, the  $i$ -th vehicle kinematics is usually nonlinear and nonholonomic, and describes the state evolution as:

$$X_i[k+1] = X_i[k] + h(X_i[k], u_i[k]) + Gw_i[k], \quad (1)$$

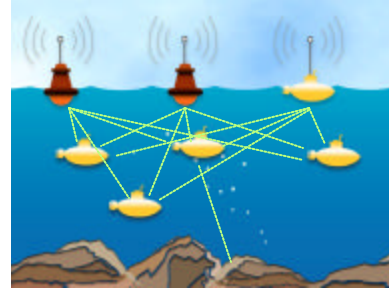
where  $U_i$  is the control input to the vehicle and  $W_i$  is state measurement noise, assumed to be white, with zero mean, and covariance matrix  $E[w_i[k]w_i[k]] = Q_i$ . Without loss of generality, we require that the  $N$  vehicles be synchronized in time at each sample point  $k$ . At each sample point the  $i$ -th vehicle measurement model is written as:

$$g(X_i[k], A[k], Y_i[k]) + \eta_i[k] = 0, \quad (2)$$

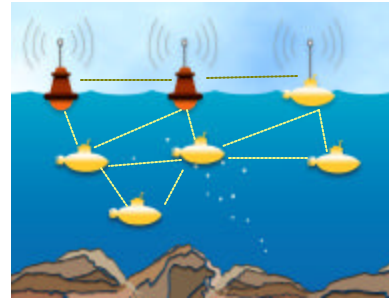
where  $g$  is a nonlinear function of the vehicle position,  $X_i[k]$ , measurements of a noisy field variable  $Y_i[k]$ , with a white noise component with zero mean and covariance matrix  $\sigma_i$ . The vector  $A$  is a set of known or unknown coefficients

describing the field variable dependence with the sample location. If the set of coefficients is unknown but constant, the vector  $A$  will be added to the overall system state, and its evolution will be governed simply by  $A[k+1] = A[k]$ .

The simultaneous sampling and navigation estimation problem reduces to estimating the overall state vector  $X[k] = (X_1[k]; \dots; X_N[k], A)$ , along with its covariance matrix  $P[k]$ .



Cooperative Mapping and Localization



Distributed Network Architecture



Multi-sensor Fusion for Distributed Fields

Fig. 7. Schematic diagram of fundamental problems related to adaptive sampling.

A solution is available using the Extended Kalman Filter (EKF) [46-48], by using Taylor expansion approximations of the nonlinear functions  $h$ , and  $g$ , and reducing the problem to a linear Kalman filter estimation problem. By the Taylor series expansion:

$$X_i[k+1] \approx \frac{\partial h(X_i[k|k], u_i[k+1])}{\partial X} (X_i[k+1] - X_i[k|k+1]) + X_i[k|k+1] + Gw_i[k],$$

$$0? g(X_i[k], Y_i[k] | k) | g(X_i[k | k-1], Y_i[k]) | \frac{?g(X_i[k | k-1], Y_i[k])}{?Y} | ?_i[k] |$$

$$? \frac{?g(X_i[k | k-1], Y_i[k])}{?X} (X_i[k] | X_i[k | k-1]),$$

$$X_i[k | k-1] | X_i[k-1] | h(X_i[k-1], u_i[k-1]).$$

If we denote

$$M_i[k] | \frac{?g(X_i[k | k-1], Y_i[k])}{?X}, ?_i[k] | \frac{?g(X_i[k | k-1], Y_i[k])}{?Y} | ?_i[k],$$

$$Z_i[k] | ?g(X_i[k | k-1], Y_i[k]) | \frac{?g(X_i[k | k-1], Y_i[k])}{?X} | X_i[k | k-1],$$

then the linearized measurement equation becomes:

$$Z_i[k] | M_i[k] X_i[k] | ?_i[k],$$

where the noise covariance is now:

$$E[?_i[k] | ?_i[k]] | \frac{?g(X_i[k | k-1], Y_i[k])}{?Y} | ?_i | \frac{?g(X_i[k | k-1], Y_i[k])^T}{?Y} | ?_i,$$

and the overall Kalman filter formulation becomes:

? Prediction of the state:

$$X_i[k | k-1] | X_i[k-1] | h(X_i[k-1], u_i[k-1])$$

? Prediction of covariance matrix:

$$P_i[k | k-1] | \frac{?h_{k?1}}{?X} P_i[k-1] | \frac{?h_{k?1}^T}{?X} | ? G Q_i G^T$$

? Kalman gain:

$$K_i[k] | P_i[k | k-1] M_i[k]^T | (M_i[k] P_i[k | k-1] M_i[k]^T | ?_i[k])^{-1},$$

? State estimation equation:

$$X_i[k] | X_i[k | k-1] | K_i[k] g(X_i[k | k-1], Y_i[k])$$

? Covariance matrix equation:

$$P_i[k] | (I | K_i[k] M_i[k]) P_i[k | k-1].$$

A common measure of uncertainty is provided by the entropy of the probability density function for the estimated state:

$$H(k) | ? ? p(x) \log(p(x)) dx, \quad (3)$$

which for a Gaussian pdf is related to the state covariance through:

$$H(k) | \frac{1}{2} \ln((2?)^d e^{\|P(k)\|}). \quad (4)$$

The effectiveness of the ASA algorithm can be found by comparing the entropy before and after a next sampling step. This could be expressed by the Kullback-Liebler divergence expressing the dissimilarity between two pdf's  $p(x)$  and  $q(x)$ . The measure of difficulty in discriminating in favor of  $p$  against  $q$  can be expressed as:

$$D(p : q) | ?_i p(x) \log(p(x)/q(x)) dx$$

and the overall measure of dissimilarity is:

$J(p, q) | D(p : q) | D(q : p)$ , which for the behavior of the  $i$ -th AUV using the EKF approach outlined below becomes:

$$J(k | 1, k) | D(P[k | 1] : P[k]) | D(P[k] : P[k | 1])$$

The Adaptive Sampling Algorithm (ASA) will then seek to sample at a new location such as to minimize the divergence function. A more intuitive measure of effectiveness for the ASA algorithm is to require that at the new sampling point for the  $i$ -th AUV such that the infinity norm of  $P_i[k | 1]$  is minimized.

### C. Localization uncertainty

Most AUVs are nonholonomic robots, and in this paper we consider an approximate kinematic model for AUSI's SAUV-II. We use this model to illustrate the vehicle localization uncertainty by using dead-reckoning. The solar AUV is driven by a steerable rear thrust vector as shown in Figure 8, and is equipped with an axial velocity sensor measuring flow along the center line of the vehicle ( $u_{||}$ ), as well as steering thrust angle measurements and a compass measuring the vehicle orientation (?). If we just consider the 2D yaw (?) model of the vehicle, e.g. the vehicle maneuvers at a constant depth, the kinematics can be written as:

$$\begin{aligned} \dot{x} &= u_1 \cos \theta \cos \psi - k u_1 \sin \theta \sin \psi \\ \dot{y} &= u_1 \cos \theta \sin \psi + k u_1 \sin \theta \cos \psi \\ \dot{\theta} &= u_2 \\ \dot{\psi} &= \frac{(1 - k)}{R} u_1 \sin \theta \end{aligned} \quad (5)$$

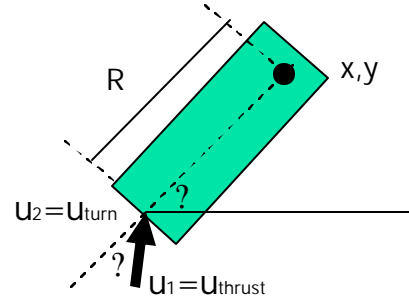


Fig. 8: A simple kinematic model for SAUV-II

The vehicle state variable is  $X = [x, y, \theta, \psi]$ , and the measured outputs are  $\theta, \psi$ , and  $u_{||} = u_1 \cos(\theta)$ . The constant  $k$  is a lateral slip coefficient for the vehicle. SAUV-II is also equipped with a GPS unit that can only be used when the vehicle is surfaced. If the vehicle sample its outputs at time intervals  $dt$ , the dead-reckoned estimate of position can be written as:

$$\hat{X}[k | 1] | \hat{X}[k] | dt (f_1(\hat{X}[k]) u_1[k] | f_2(\hat{X}[k]) u_2[k]),$$

and the state covariance matrix becomes:

$$P[k | 1] | E[(X[k | 1] | \hat{X}[k | 1])(X[k | 1] | \hat{X}[k | 1])^T]$$

where  $X[k+1]$  is the updated dead-reckoned position of the vehicle including incremental measurement noise:

$$\begin{aligned} X[k+1] &= X[k] + dt(f_1(X[k]) + dX[k])u_1[k] \\ &+ f_2(X[k]) + dX[k]u_2[k] + X[k] + dtu_1[k]f_1(X[k]) \\ &+ dtu_2[k]f_2(X[k]) + dt(u_1 \frac{\partial f_1}{\partial X} + u_2 \frac{\partial f_2}{\partial X})dX[k]. \end{aligned}$$

Therefore,  $P[k+1] = (I + J[k])P[k](I + J[k]^T)$ , where

$$J[k] = dt(u_1[k] \frac{\partial f_1(\hat{X}[k])}{\partial X} + u_2[k] \frac{\partial f_2(\hat{X}[k])}{\partial X}). \quad (6)$$

When the vehicle is on the surface, the estimate of position can be set to the approximate steady state solution of the Kalman filter, which fuses the GPS data with the dead-reckoning information by weighting the data commensurate to its uncertainty. Evidently, if the dead-reckoning estimate is very imprecise, then its weight in the equation below is almost zero:

$$\begin{aligned} \hat{X} &= w_1 \hat{X}_{k \text{ dead/reckoning}} + w_2 \hat{X}_{GPS}, \\ w_1 &= \frac{\|P(\hat{X}_{GPS})\|_2}{\|P(\hat{X}_{GPS})\|_2 + \|P(\hat{X}_{k \text{ dead/reckoning}})\|_2}, \quad (7) \\ w_2 &= \frac{\|P(\hat{X}_{k \text{ dead/reckoning}})\|_2}{\|P(\hat{X}_{GPS})\|_2 + \|P(\hat{X}_{k \text{ dead/reckoning}})\|_2} \end{aligned}$$

Assuming that the AUV moves between way-points at maximum thrust speed, the on-board controller will chart a course that tries to follow a straight line to the destination. An example of such a controlled uses a PID gain between the estimate of the AUV heading and the desired heading:

$$\begin{aligned} u_1 &= \max\_speed, u_2 = PID(\hat{\theta}_d - \hat{\theta}), \quad (8) \\ \hat{\theta}_d &= a \tan 2(x_d - \hat{x}, y_d - \hat{y}) \end{aligned}$$

To illustrate the fact that dead-reckoning by itself can introduce a very large error if GPS measurements are not used frequently enough, we simulated a ‘‘U’’ maneuver for the SAUV. The dead-reckoning estimate of the final AUV position was obtained by integrating the nominal kinematics, while the ‘‘truth’’ model was obtained by using a 10% vehicle thrust error, and a 1 degree compass uncertainty. The results shown in Figure 9, indicate that the vehicle would be approximately 30m off course, if it does not surface at various way-point locations during the maneuver. This model forms the basis for adaptive sampling analysis under true mission conditions, and will be utilized in further mission planning development.

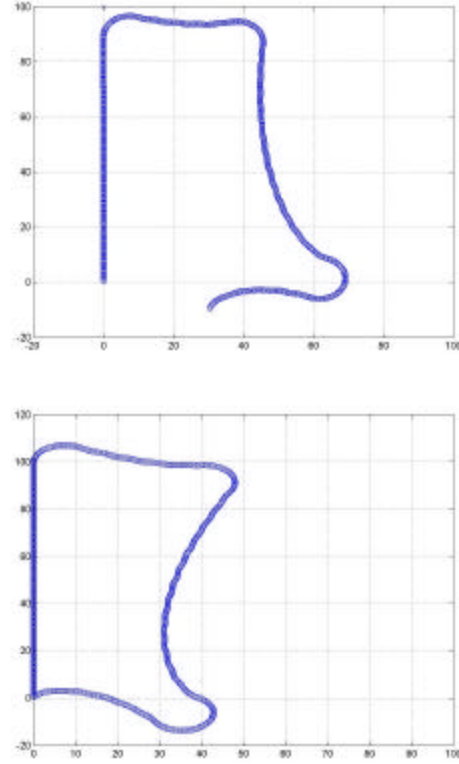


Fig 9. Actual course (top) and dead-reckoned course (bottom) of the nonholonomic AUV model (5), with a 5m turn radius, using the closed loop feedback scheme (8).

#### D. Concurrent localization and estimation for a linear field

In this section we illustrate the proposed ASA for field estimation using a linear measurement function. The assumption that the field distribution is linear will allow us to compute a closed form solution for the information measure used by the ASA algorithm. The sampling objective is to determine the unknown coefficients of the 3D plane that describes the field variable.

Using a 2-dimensional yaw-only kinematic model, and assuming that the sensed variable is distributed linearly with the 2D position  $(x,y)$ , the EKF model equations for a single vehicle can be written as:

$$\begin{aligned} x_{k+1} &= x_k + h(f_{11}(\theta_k, w_k, u_1)) + f_{12}(\theta_k, w_k, u_2) \\ y_{k+1} &= y_k + h(f_{21}(\theta_k, w_k, u_1)) + f_{22}(\theta_k, w_k, u_2) \\ a_{k+1} &= a_k, X_k = \begin{bmatrix} x_k \\ y_k \\ a_k \end{bmatrix}, Y_k = X_k^T a_k \\ \text{var}(w_k) &= Q_k, \text{var}(\theta_k) = \sigma_k \end{aligned} \quad (9)$$

The system state contains the vehicle latitude and longitude, as well as the three unknown field coefficients. The problem reduces to estimating the coefficients of a linear

regression function from field variable measurements, and we can reduce the problem to the following linearized form:

$$\begin{aligned} Z_k &= M_k s_k + \eta_k, M_k = (a_{k|k-1}^T \quad X_{k|k-1}^T) \\ Z_k &= Y_k + X_{k|k-1}^T a_{k|k-1} \\ \eta_k &= \text{noise} \end{aligned} \quad (10)$$

Since both the vehicle position as well as the unknown field coefficients are part of the estimator state, the measurement equation is nonlinear and it has to be approximated using the Taylor expansion. However, we could also obtain a closed form for the covariance matrix of the estimated field coefficients from the least-square solution. Since the first n measurements obey the following linear relation:

$$\begin{aligned} Z_1 &= a_1 + a_2 x_1 + a_3 y_1 \\ Z_2 &= a_1 + a_2 x_2 + a_3 y_2 \\ &\vdots \\ Z_n &= a_1 + a_2 x_n + a_3 y_n \end{aligned} \quad (11)$$

we can directly estimate the unknown coefficients from:

$$\hat{A}_n = (X^T X)^{-1} X^T Z \quad (12)$$

Furthermore, because the pseudo-inverse has a closed form  $M_n^+ = (M_n^T M_n)^{-1} M_n^T$ , we obtain:

$$\hat{A}_n = (M_n^T M_n)^{-1} M_n^T Z \quad (13)$$

We first pose the estimation problem in the absence of any navigational errors, i.e., we assume that the sample locations  $X_i[k]$  are known accurately. Due to GPS, this is a reasonable assumption to make if the samples are taken at points where the vehicle surfaces. The covariance matrix of  $\hat{A}_n$  can now be related directly to the (constant) measurement uncertainty as:

$\text{var}(\hat{A}_n) = \text{var}(Z_i) (M_n^T M_n)^{-1}$ , therefore the ASA algorithm will move the vehicle from location  $(x_n, y_n)$  to  $(x_{n+1}, y_{n+1})$ , such that the following infinity norm is maximized over the search space :

$$m(x, y) = \left\| \begin{bmatrix} 1 \\ M_n^T x \\ y \end{bmatrix} \right\|_\infty, \quad (14)$$

$$m(x_{n+1}, y_{n+1}) = m(x, y), \quad (x, y) \in \mathcal{S}$$

If the navigational errors cannot be assumed to be zero, such as in the case of dead-reckoning, we can still express the

variance of the coefficients in the closed form by noticing that if we take successive row differences we obtain:

$$\text{var} \begin{bmatrix} a_2 \\ a_3 \end{bmatrix} = \text{var} \begin{bmatrix} Z_2 - Z_1 \\ Z_3 - Z_2 \\ \vdots \\ Z_n - Z_{n-1} \end{bmatrix} = \text{var} \begin{bmatrix} a_2 \\ a_3 \end{bmatrix}$$

where  $x_i = x_i - x_{i-1}, y_i = y_i - y_{i-1}, z_i = z_i - z_{i-1}$  now have a covariance independent of the index i. Figure 10 shows the sequence of sampling points for one AUV in a 2D space represented by a 10x10 square grid, that was obtained by minimizing  $m(x,y)$  over all the unvisited points.

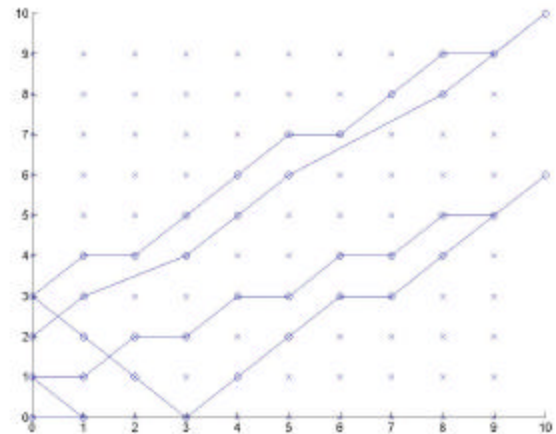


Fig 10. Sampling sequence generated by minimizing the uncertainty estimate of a linear field.

Because the SAUV is a nonholonomic system with a fixed minimum turn radius, a trajectory such as the one shown in Figure 10 violates the constraints. Instead of searching to maximize  $m(x,y)$ , we can limit the search space as follows: if the SAUV is at grid location  $(x_n, y_n)$ , find the next best sampling point on the grid to be  $(x_{n+1}, y_{n+1})$  among immediate neighbors (greedy), or among the next N-hops (finite horizon graph search) that minimizes the variance. We can further restrict the neighbors to only feasible transition rules dictated by the minimum turning radius as shown in Figure 11.

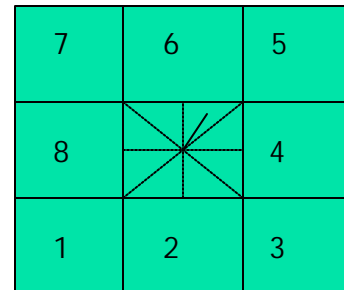


Fig 11. If SAUV heading is in the octant shown, then only allow transitions to neighboring cells 5 and 6 (if not visited), where the cell size is equal to the minimum turning radius of the vehicle

The resulting trajectory shows a path that avoids sharp vehicle turns, as shown in Figure 12.

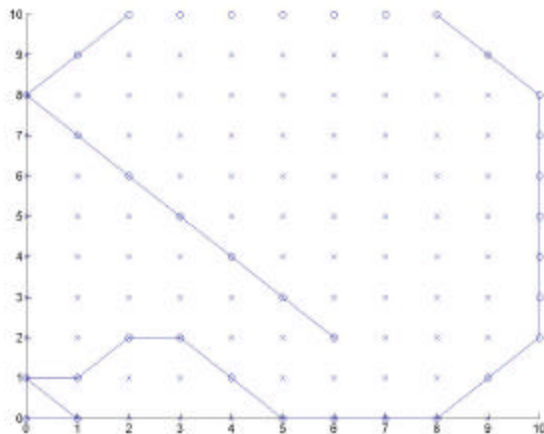


Fig 12. Sampling sequence generated by minimizing the uncertainty estimate of a linear field, while taking into account the nonholonomic constraints of the vehicle.

## V. COMMUNICATION CONSTRAINTS

Communication between AUVs is another essential component for any sampling mission. In this section we formulate the network model for a set of  $N$  multiple AUVs based on previous work from congestion control. The AUVs form the nodes in an ad-hoc network, and they communicate through a wireless RF signals when the vehicles are surfaced, and acoustic modems when they are submerged. The flow control problem through an ad-hoc network can be further separated into two problems: a routing problem, and a congestion control problem. The “routing problem” is similar to a “traveling salesman” NP-hard problem in that it aims to select data routes (“hops”) with minimal cost between the nodes. The “cost” can be defined in terms of geographical distance, energy consumed, or time delay through the network. Because it is NP hard, many solutions based on heuristics have been proposed [3,21,27].

The “congestion control problem” consists of finding and regulating the optimal flow rates between the network nodes in the presence of network capacity constraints. This problem can be further decomposed into a static optimization problem and a dynamic stabilization problem. Typically, solutions to both the routing and congestion control problems are differentiators between different network protocols, but we will assume that the communication hardware provided to the robot nodes has been a-priori chosen.

Here we focus on sampling problems that combine navigation and communication of multiple AUVs. Highly desirable attributes for this architecture would be decentralization, so that individual AUVs would be able to operate independently, or only with localized knowledge. Another important attribute is that it can be scaled to large numbers AUVs.

We formulate the sampling algorithm with communication constraints by using the so-called utility function of the network. Specifically, we would like to control individual robot location ( $r_i$ ), and its sensor data rate ( $x_i$ ) over time in order to maximize a combined potential function

$$U = \prod_{i=1}^N (U_{1i}(r_i, r_{goal}, r_{obstacle}) \cdot U_{2i}(x_i, r_i)). \quad (15)$$

Network flow control regulates the flow of data between sources and links based on congestion. Keeping notations consistent with [7], a relationship is established between each of the sources with data rates ( $x_i$ ) and the individual links with data rates ( $y_l$ ) by the routing matrix,  $R: y = Rx$ .

Each of the links has a maximum capacity value given by  $c_l$ . In our case, the source rates are sensor readings from individual AUVs, and the link rates are aggregate source rates forwarded by the network based on its routing scheme. The static optimization of the network flow control problem consists of maximizing a utility (or utilization) function for all of the sources using fixed capacity constraints.

$$\max_{x \geq 0} \prod_{i=1}^N U_i(x_i) \quad \text{subject to } Rx \leq c. \quad (16)$$

where  $U_i$  is a strictly concave utility function and  $R$  is the routing matrix for the network [7]. The concave/convex requirement for  $U_i$ , combined with a full row rank condition of the routing matrix  $R$  are sufficient (but not necessary) conditions to ensure that there exists a unique minimum solution to the associated constrained optimization problem (3). Various utility functions are used for different network models, for example  $\arctan(x_i)$  for TCP Reno and  $\log(x_i)$  for TCP Vegas [6].

The congestion control problem consists of setting both the source and link controls of the network to ensure that the data rates and node buffers remain stable and converge to their static optimal values. For simplicity, in this paper we ignore the dynamic feedback stabilization problem for the network and assume that the optimal source rates are observed. We also assume that the network protocol is given a-priori, and that we only have access to modifying the node data rate as part of our optimization strategy.

As a reflection of the network mobility, however, we assume that the link capacity constraints can vary with the distance between network nodes. This is consistent with Shannon’s theorem that predicts that the maximum achievable data rate between two nodes is given by:

$$C = W \log_2 \left( 1 + \frac{K P_t}{W N_o d^\alpha} \right) \quad (17)$$

where  $P$  is the power,  $d$  is the distance between nodes,  $W$  is the bandwidth,  $\alpha$  is the path loss coefficient,  $F$  is the fading margin,  $K$  is the propagation constant dependent on the

medium, and  $K \propto K'F$  [1]. Equation (17) breaks down as  $d$  shrinks to zero, since node to node communication rates is limited by the on-board processing capabilities. A slightly different model is used instead, namely:

$$C = \begin{cases} c_o \left( \frac{1}{d} - \frac{1}{r_{zone}} \right), & r_{min} \leq d \leq r_{zone} \\ c_o \left( \frac{1}{r_{min}} - \frac{1}{r_{zone}} \right), & d \leq r_{min} \\ 0, & d \geq r_{zone} \end{cases}, \quad (18)$$

with a profile shown in Figure (13).

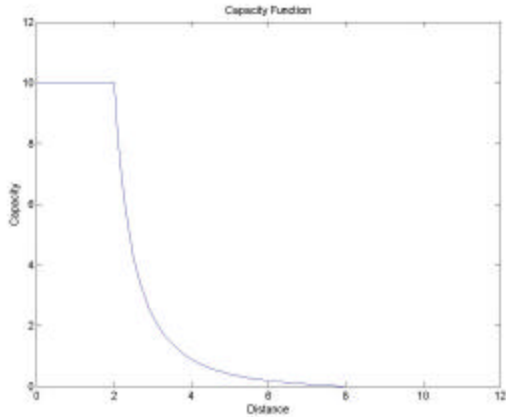


Fig. 13: Link capacity as a function of its distance with  $a=2$ ,  $r_{zone} = 8$ ,  $r_{min} = 2$ .

Because the data rate varies with distance between nodes, the optimal utility function value will also vary with node location, as the solution of an unconstrained optimization problem using Lagrange multipliers:

$$U^*(r_{i \in \{1, N\}}) = \min_{p_l \geq 0} \max_{x_i \geq 0} \left( \sum_{i \in \{1, N\}} w_i U(x_i) - \sum_{l \in \{1, L\}} p_l (c_l(r_i) - y_l) \right).$$

In a classical network formulation, the utility functions of each node are equally weighed. By using different but non-zero, positive weights  $w_i$  (to maintain convexity), we can differentiate between task defined important and not so important nodes in the network. Since we assume that the network protocol is given, routing will ultimately be determined by the chosen protocol. An example of such a protocol for underwater networks is AUSNET [43], developed by AUSI for multiple Solar AUVs. For simulation purposes, however, we implemented a routing scheme based on a balanced depth first search of the fully connected graph formed between the robot node locations. This scheme is similar to a modified version of the Zone Routing Protocol (ZRP) found in [3]. ZRP creates a circular zone around each node of radius parameter  $r_{zone}$ . Within each zone, the center node knows the geographical topology of the network within that radius (i.e. it knows the nodes located inside that

perimeter and the distance to these nodes). This knowledge could be based on triangulation range measurements, dead reckoning, cooperative localization, etc. An example of such a routing configuration is shown in Figure 14.

## VI. POTENTIAL FIELDS

### A. Node Equations of Motion

In the context of robot navigation, the potential field method creates a vector field representing a navigational path based on a potential function. These vectors then act as artificial forces upon the nodes resulting in motion through a dynamic equation of motion. The first approach to obstacle avoidance using the potential field approach was by Krogh [4]. In a somewhat limited way, the potential field method has been extended to mobile sensor network deployment in [1] by using artificial repelling forces to steer the robots towards a state of equidistant equilibrium.

Given a scalar potential field function  $U(r)$  that depends on the robot position, one can calculate forces governing the robot motion of based on the gradient of the scalar potential field:

$$\mathbf{F} = -\nabla U(\mathbf{r}) \quad (19)$$

In this paper we consider the following actuating forces for the mobile sensor network:

1) Attractive forces towards goals. The goal points are waypoints or sampling locations provided by the ASA algorithm. In our simulations, these forces are simple attractors to single or multiple points a 2D space:

$$\mathbf{F}_{i,goal} = w(\mathbf{r}_i - \mathbf{r}_{goal})$$

2) Repulsive forces given by obstacles and other robots. In our simulations, these forces are caused by rolling down a potential “hill” with a single top centered inside the object:

3) Attractive forces based on maximizing capacity between nodes.

$$\mathbf{F}_i = \frac{\nabla U^*}{r_i}, \text{ where } U^* \text{ is the optimal value of the communication utility function.}$$

4) Attractive “restoring” forces based on penalties for exceeding the maximum allowable communication distance between nodes:

$$\mathbf{F}_{restore}(i, j) = u_{ij}(\mathbf{r}_j - \mathbf{r}_i)$$

After the force calculation, the equation of motion for the  $i$ -th sensor node will be given by integrating a simple mass-damper model over time:

$$m_i \ddot{\mathbf{r}}_i + \nu_i \dot{\mathbf{r}}_i = \mathbf{F}_i, \quad (20)$$

where  $m$  and  $\nu$  are mass and damping terms respectively. Note that these terms have no physical meaning, and they are only used to define a dynamic equation of motion for the system in the direction of the gradient of a global potential field function consisting of obstacles, goal locations, and

network utility. The motion of the robots stops when a minimum energy configuration is reached. Because the minimum could be local and not global, time varying attractive forces related to the goal, or other annealing methods could be introduced.

### B. Energy consumption

Considerations of energy minimization are important in ensuring the maximum lifetime of the mobile sensor network before its batteries need to be recharged. In a typical meso-robot/wireless radio configuration, the node energy consumption due to computation is in microwatt range, to communication in mW to hundreds of mW range, and to motion (hundreds of mW to tens of W). Because the energy expended to move the robot is likely to exceed the other power required for the other subsystems, we would like to incorporate an energy minimization term in the robot equations of motion. One way to achieve is by adding an additional motion energy term in the overall potential function we are minimizing. Another, much simpler way, is to make individual damping coefficients vary with the amount of motion energy expanded as shown below:

$$k_{\gamma_i}(t) = k_{\gamma_i} \left( 1 - \frac{E_i(t)}{E_o} \right) \quad (9)$$

If the robot node damping increases with expended motion energy, or alternatively, it decreases with the amount of on-board energy available, the robot speed decreases accordingly. As a result, the available energy will not drain to zero and the node can remain useful as a network node. The simulation results show that:

1. Rerouting (forced after every 10 iterations) will significantly alter the network flow if the nodes are moving.
2. The nodes that are not involved with goal attainment or routing of sensory data from the robots near the goal will slowly drift towards the sink node (e.g. node 20 at (0,0)). This is expected due to the attractive nature of the network forces.
3. If no energy-damping coefficient is used, or if it is 1.0 the goal is attained or nearly attained after 100 iterations. If the coefficient is 10.0 the goal is not attained.
4. The individual energy consumption per node decreases as the damping coefficient increases, being the highest for  $k_{\gamma_i} \rightarrow 0$ , and the lowest for  $k_{\gamma_i} \rightarrow 10$ . We conclude that the goal attainment time can be balanced with the per-node energy consumption by varying the energy dependent damping coefficient.

An example of a reconfiguration simulation for a network with 20 AUVs is shown in Figure 14. Further details of the potential field algorithm are presented in [51].

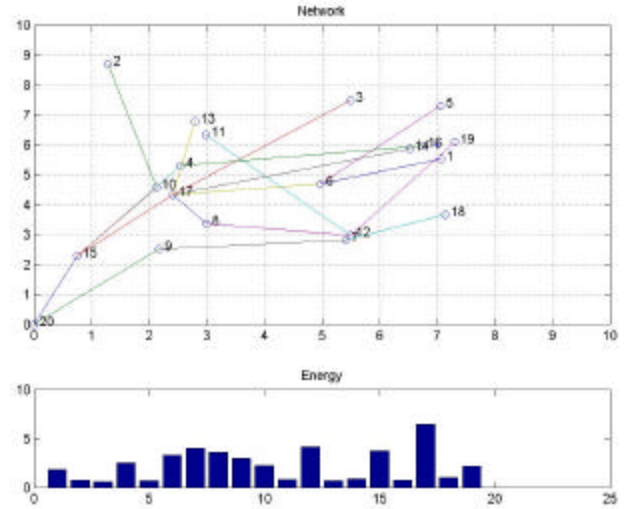


Figure 14: 20 node configuration and energy after 100 iterations with a 1.0 energy-dependent damping coefficient.

## VII. CONCLUSION AND FUTURE WORK

In this paper we formulated an estimation-based approach for the problem of adaptive sampling using multiple AUVs. Secondary objectives such as energy and communication bandwidth optimization are introduced using a potential fields approach. The underwater vehicles are directed to sample at locations that most reduce the uncertainty in our knowledge of the field distribution.

Future work includes expanding the simulation work to non-linear varying field distribution and different localization algorithms. In parallel, we will carry out experiments in mapping dissolved oxygen, bathymetry, and other field distributions using multiple Solar AUVs. Finally, the effectiveness of our sampling strategy will be quantitatively evaluated in both simulation and experiments.

### ACKNOWLEDGEMENTS

This work was partially funded by a grant from the National Science Foundation Grant #IIS-0329837. We wish to thank Chad Helm and Vadiraj Hombal for their contributions to this work.

### REFERENCES

- [1] M. J. Mataric A. Howard and G. S. Sukhatme, "Mobile sensor network deployment using potential fields: A distributed, scalable solution to the area coverage problem," in Proceedings of the 6th Int'l Symposium on Distributed Autonomous Robotics Systems, 2002.
- [2] V. Kumar G. A. S. Pereira, A. K. Das and M. F. M. Campos, "Decentralized motion planning for multiple robots subject to sensing and communications constraints," in Proceedings of the Second Multi Robot Systems Workshop, 2003.
- [3] Z. J. Haas, "A new routing protocol for the reconfigurable wireless networks," in IEEE International Conference on Universal Personal Computing, 1997.

- [4] B. H. Krogh, "A generalized potential field approach to obstacle avoidance control," in *Robotics Research: The Next Five Years and Beyond*, Society of Manufacturing Engineers, 1984.
- [5] F. Michaud and E. Robichaud, "Sharing charging stations for long-term activity of autonomous robots," in *Proc. IEEE International Conference on Intelligent Robots and Systems*, 2002.
- [6] F. Paganini S.H. Low and J. C. Doyle, "Internet congestion control," in *IEEE Control Systems Magazine*, 2002.
- [7] J. T. Wen and M. Arcak, "A unifying passivity framework for network control", to appear in *IEEE Trans. on Automatic Control*, 2004.
- [8] T. G. Sugar and V. Kumar, "Control of cooperating mobile manipulators", in *IEEE Transactions on Robotics and Automation*, 18(1):94-103, February 2002.
- [9] W. Burgard, M. Moors, D. Fox, R. Simmons, and S. Thrun., "Collaborative multi-robot exploration," in *Proc. of IEEE International Conference on Robotics and Automation*, volume 1, pages 476-81, 2000.
- [10] D. W. Gage., "Command control for many-robot systems," in *AUVS-92, the Nineteenth Annual AUVS Technical Symposium*, pages 22-24, Huntsville Alabama, USA, June 1992. Reprinted in *Unmanned Systems Magazine*, Fall 1992, Volume 10, Number 4, pp 28-34.
- [11] A. Howard, M. J. Mataric, and G. S. Sukhatme, "Localization for mobile robot teams: A maximum likelihood approach," Technical Report IRIS-01-407, Institute for Robotics and Intelligent Systems Technical Report, University of Southern California, 2001.
- [12] R. Simmons, D. Apfelbaum, W. Burgard, D. Fox, M. Moors, S. Thrun, and H. Younes, "Coordination for multi-robot exploration and mapping," in *Proc. of the Seventeenth National Conference on Artificial Intelligence (AAAI-2000)*, pages 852-858, 2000.
- [13] B. Yamauchi, "Frontier-based approach for autonomous exploration," in *Proceedings of the IEEE International Symposium on Computational Intelligence, Robotics and Automation*, pages 146-151, 1997.
- [14] Ronald C. Arkin, **Behavior-Based Robotics (Intelligent Robotics and Autonomous Agents)**, MIT Press, May 22, 1998.
- [15] J.W. Fenwick, P. M. Newman, J.J. Leonard, "Cooperative Concurrent Mapping and Localization," in *Proc. of the IEEE Int'l Conf. on Robotics and Automation*, May 2002.
- [16] S.T. Pfister, K.L. Kriechbaum, J.W. Burdick, "Weighted range sensor matching algorithms for mobile robot displacement estimation", in *Proc. of the IEEE Int'l Conf. On Robotics and Automation*, May 2002.
- [17] A. Howard, M. J. Mataric, and G. S. Sukhatme, "An incremental Self-Deployment Algorithm for Mobile Sensor Networks", in *Autonomous Robots 13*, pp. 113-126, 2002.
- [18] L. E. Parker, B. Kannan, X. Fu, and Y. Tang, "Heterogeneous Mobile Sensor Net Deployment Using Robot Herding and Line-of-Sight Formations", in *Proceedings of IEEE International Conference on Intelligent Robots and Systems*, 2003.
- [19] D. Popa, J. Wen, "Nonholonomic Path-Planning with Obstacle avoidance", in *Proc. Int'l Conference in Robotics and Automation*, Minneapolis, April 1996.
- [20] J. Latombe, "Robot Motion Planning", Kluwer Academic Publishers, MA, 1991.
- [21] N. Hutin, C. Pegard, E. Brassart, "A Communication Strategy for Cooperative Robots", in *Proc. 1998IEEE/RSJ Int'l Cong. On Intelligent Robots and Systems*, Oct. 1998.
- [22] P. Gupta, and P.R. Kumar, "The Capacity of Wireless Networks", in *IEEE Transactions on Information Theory*, vol. 46, No.2, March 2000.
- [23] J. Cortes, S. Martinez, T. Karatas, and F. Bullo, "Coverage control for mobile sensor networks", in *IEEE Trans. On Robotics and Automation*, 2002.
- [24] W. Ye, J. Heindemann, D. Estrin, "An Energy-Efficient MAC Protocol for Wireless Sensor Networks", in *Proc. of INFOCOM 2002*.
- [25] Yan Yu, R. Govindan, and D. Estrin, "Geographical and Energy Aware Routing: a recursive data dissemination protocol for wireless sensor networks", USC Computer Science Department Technical Report TR01-745, May 2001.
- [26] A. Zelinsky, R. A. Jarvis, J.C. Byrne and S. Yuta, "Planning Paths of Complete Coverage of an Unstructured Environment by a Mobile Robot", in *Proc. Int'l Conf. On Advanced Robotics (ICAR)*, 1993.
- [27] Q. Li, R. Peterson, M. DeRosa, and D. Rus, "Reactive Behavior in Self-Reconfiguring Sensor Networks", in *Proc. MOBICOM '02*, Sept 2002.
- [28] Thompson, Steven K., **Sampling**. John Wiley and Sons, Inc., New York, 1992.
- [29] Thompson, Steven K, and George A.F. Seber, **Adaptive Sampling**. John Wiley and Sons, Inc., New York, 1996.
- [30] Brink, K.H., "Observational coastal oceanography, Advances and Primary Research Opportunities in Physical Oceanography Studies", (APROPOS) Workshop, NSF-sponsored workshop on the Future of Physical Oceanography, 15-17 December, 1997.
- [31] Creed, E.L., S.M. Glenn and R. Chant, "Adaptive Sampling Experiment at LEO-15", 1998.
- [32] Curtin, T.B., J.G. Bellingham, J. Catipovic and D. Webb, 1993. "Autonomous ocean sampling networks", *Oceanography*, 6(3), pp. 86-94.
- [33] Glenn, S.M., G.Z. Forristall, P. Cornillon and G. Milkowski, 1990. "Observations of Gulf Stream Ring 83-E and Their Interpretation Using Feature Models", *Journal of Geophysical Research*, 95, 13,043-13,063.
- [34] Keen, T.R. and S.M. Glenn, "Factors influencing hindcast skill for modeling shallow water currents during Hurricane Andrew", *J. Atmos. Ocean. Tech.*, 15, pp. 221-236.
- [35] Robinson, A.R., "Forecasting and simulating coastal ocean processes and variabilities with the Harvard Ocean Prediction System", in *Coastal Ocean prediction*, (C.N.K. Mooers, ed.), AGU Coastal and Estuarine Studies Series, American Geophysical Union, pp. 77-100.
- [36] Robinson, A.R., J.A. Carton, N. Pinardi and C.N.K. Mooers, "Dynamical forecasting and dynamical interpolation: an experiment in the California Current", *Journal of Physical Oceanography*, 16: 1561-1579.
- [37] D. Richard Blidberg, "The Development of Autonomous Underwater Vehicles (AUVs); A Brief Summary", ICRA, Seoul, Korea, May 2001.
- [38] D. Richard Blidberg, "Solar Powered Autonomous Undersea Vehicles", *Sea Technology* 1997.
- [39] D. Richard Blidberg, et.al., "Results of the Evaluation and Testing of the Solar Powered AUV and its Subsystems", UUST99.
- [40] Steven G. Chappell, et.al., *Autonomous Undersea Systems Institute, "Cooperative AUV Development Concept (CADCON) An Environment for High-Level Multiple AUV Simulation"*, UUST99.
- [41] R. K. Rew, G. P. Davis, and S. Emmerson, "NetCDF User's Guide: An Interface for Data Access", Version 2.3, University Corporation for Atmospheric Research, Boulder, Colorado, April 1993.
- [42] Sai S. Mupparapu, et.al., "Autonomous Systems Monitoring and Control (ASMAC) - An AUV Fleet Controller", in *Proc. Autonomous Underwater Vehicles Workshop, AUV'04*, July 2004.
- [43] Charles J. Benton, James Kenney, Sai Sharan Mupparapu, Robert Nitzel, "Autonomous Undersea Systems Network: Protocols for Ad-Hoc Undersea Networks", in *Proc. Autonomous Underwater Vehicles Workshop, AUV '04*, July 2004.
- [44] A. Bennet, *Inverse Modeling of the Ocean and Atmosphere*, Cambridge Press, 2002.
- [45] J. Sasiadek, Q. Wang, R. Johnson, L. Sun, J. Zalewski, "UAV Navigation Based On Parallel Extended Kalman Filter", *AIAA Guidance, Navigation and Control Conference Denver, Colorado*, August 14-17, 2000.
- [46] Gelb, A. (Ed.), **Applied Optimal Estimation**, The MIT Press, Cambridge, Mass., 1974.
- [47] Lewis, F.L., **Optimal Estimation with an Introduction to Stochastic Control Theory**, John Wiley and Sons, New York, 1986.
- [48] Brown, R.G., P.Y.C. Hwang, **Introduction to Random Signals and Applied Kalman Filtering**, 3rd Edition, John Wiley and Sons, New York, 1997.
- [49] Jochen, P., W. Meyer-Hilberg, T. Jacob, "High Accuracy Navigation and Landing System using GPS/IMU System Integration", 1994 IEEE Position Location and Navigation Symposium, pp. 298-305.
- [50] A.C. Sanderson, "Multirobot Navigation Using Cooperative Teams", *Distributed Autonomous Robotic Systems*, pp. 389-400, Springer-Verlag, Asama et.al. eds, 1998.
- [51] D. O. Popa, et.al., "Robotics Deployment of Sensor Networks Using Potential Fields", in *Proc. Int'l Conf. on Robotics and Automation, ICRA '04*, New Orleans, April 2004.
- [52] Feng Zhao, et.al., "Collaborative Signal and Information Processing: An Information\_Directed Approach", in *Proc of the IEEE*, vol. 91, no. 8, August 2003.